Catalysis Science & Technology

Accepted Manuscript

This article can be cited before page numbers have been issued, to do this please use: F. Cai, W. Zhu and G. Xiao, *Catal. Sci. Technol.*, 2016, DOI: 10.1039/C6CY00085A.

ROYAL SOCIETY OF CHEMISTRY

www.rsc.org/catalysis

Journal Name

View Article Online
DOI: 10.1039/C6CY00085A

ARTICLE

Promoting effect of zirconium oxide on Cu-Al_2O_3 catalyst for the hydrogenolysis of glycerol to 1,2-propanediol

Received 00th January 20xx,
Accepted 00th January 20xx

DOI: 10.1039/x0xx00000x

www.rsc.org/

Fufeng Cai, Wei Zhu and Guomin Xiao*

In this work, the ZrO_2-promoted Cu-Al_2O_3 catalysts prepared by co-precipitation method were used for the hydrogenolysis of glycerol to 1,2-propanediol in a fixed-bed reactor. These catalysts were fully characterized by BET, ICP, N_2O chemisorption, XRD, H_2-TPR, NH_3-TPD, XPS, TEM and TGA. The relationship between the catalytic activity and metal-support interaction was studied in detail. The experiment results showed that addition of ZrO_2 to Cu-Al_2O_3 could greatly enhance glycerol conversion and 1,2-propanediol selectivity. This improvement was related to the increases in the acidity and Cu dispersion on the catalytic surface. The optimal 20ZrCu-Al_2O_3 catalyst attained 97.1% glycerol conversion and 95.3% 1,2-propanediol selectivity. Furthermore, the effects of process parameters like solvent, reaction temperature, operating pressure, glycerol concentration and liquid flow rate on glycerol hydrogenolysis together with the catalyst stability were deeply investigated. Compared with Cu-Al_2O_3 catalyst, the ZrO_2-promoted Cu-Al_2O_3 catalyst had better stability and prospective for practical application, which was likely due to the high Cu dispersion and strong interaction between copper and zirconium species.

1. Introduction

In the last decades, increasing environmental issues and declining petroleum resources have encouraged the development of biofuels.[1] In this context, biodiesel produced by transesterification reaction has received significant interest because of its renewable and environmental-friendly property. However, large amounts of glycerol are simultaneously generated as a by-product in the production of biodiesel. Converting the oversupplied glycerol to valuable chemicals can effectively enhance the added value of the biodiesel. For this reason, several routes have been proposed for the transformation of glycerol to different chemicals by catalytic processes.[2] In particular, much efforts have been focused on the hydrogenolysis of glycerol to 1,2-propanediol (1,2-PDO) which is widely applied in the manufacture of the important chemicals such as cosmetics, pharmaceuticals, functional fluids, and polyesters resins.[3] Nevertheless, 1,2-PDO at present is mainly produced from petroleum derivates. Thus, the production of 1,2-PDO from glycerol has attracted considerable attention in academia and industry because this process provides a sustainable route for the production of 1,2-PDO.

A variety of heterogeneous catalysts based on noble metals and non-noble metals have been used for the hydrogenolysis of glycerol to 1,2-PDO in recent years.[4–12] Particularly, because of their lower ability to cleave C-C bond and high efficiency for C-O bond hydrogenolysis, various Cu-based catalysts such as Cu/Al_2O_3, Cu/ZrO_2, Cu/ZnO, Cu/SiO_2, and Cu/MgO have been selected to glycerol hydrogenolysis.[13–16] Nevertheless, there are still some drawbacks such as poor catalytic activity and stability for the Cu-based catalysts that need to be overcome.[12,13]

It is well documented that the acidity of the catalyst has greatly impact on the glycerol conversion.[4,17] On the other hand, suitable acid components are necessary for glycerol hydrogenolysis on the basis of the dehydration-hydrogenation reaction mechanism.[18,19] Thus, modification of Cu-based catalysts by the promoter with an appropriate acidity will help to improve the catalytic activity for glycerol hydrogenolysis. Recently, the strong acidic nature of ZrO_2 has been fully discussed in the literature.[20,21] Raju et al.[22] published the ZrO_2-based catalysts were responsible for the acetol produced from glycerol which could further undergo hydrogenation reaction and produce 1,2-PDO. Sharma et al.[23] performed that the ZrO_2-promoted Cu/ZnO/Cr_2O_3 catalysts had high Cu dispersion with suitable acidity and showed the superior catalytic activity for glycerol hydrogenolysis. However, no literature has been reported concerning ZrO_2-promoted Cu-Al_2O_3 catalysts for glycerol hydrogenolysis.

In this work, the ZrO_2-promoted Cu-Al_2O_3 catalysts prepared by co-precipitation method were used for the hydrogenolysis of glycerol to 1,2-PDO in a fixed-bed reactor. The catalysts developed in this study were well characterized by different techniques. The physicochemical properties of catalysts were correlated with the obtained catalytic performance. Further, the effects of different process parameters such as solvent, reaction temperature, operating pressure, glycerol concentration and liquid flow rate on glycerol hydrogenolysis together with the catalyst stability were investigated in detail.

School of Chemistry and Chemical Engineering, Southeast University, Nanjing 211189, China. E-mail address: xiaogm@seu.edu.cn. Tel./Fax: +86 25 52090612.
† Footnotes relating to the title and/or authors should appear here.
Electronic Supplementary Information (ESI) available: [details of any supplementary information available should be included here]. See DOI: 10.1039/x0xx00000x

2. Experimental

2.1. Chemicals and materials

Glycerol (99.0 wt.%), ethylene glycol (99.0 wt.%), methanol (99.5 wt.%), ethanol (99.7 wt.%), 1-propanol (99.0 wt.%), 2-propanol (99.7 wt.%), $Cu(NO_3)_2{\cdot}3H_2O$ (99.0 wt.%), $Al(NO_3)_3{\cdot}9H_2O$ (99.0 wt.%) and K_2CO_3 (99.0 wt.%) were obtained from Sinopharm Chemical Reagent Co., Ltd., Shanghai, China. 1,2-Propanediol (99.5 wt.%), 1,3-propanediol (99.5 wt.%), acetol (90.0 wt.%), 1,4-butanediol (99.5 wt.%) and $ZrO(NO_3)_2{\cdot}xH_2O$ (99.5 wt.% metal) were purchased from Aladdin Industrial Corporation, Shanghai, China. Hydrogen and nitrogen of high purity (≥99.99%) were obtained from Nanjing special gas factory Co., Ltd., Nanjing, China and were used directly in this work from the cylinders.

2.2. Catalyst preparation

The ZrO_2-promoted Cu-Al_2O_3 catalysts were prepared by co-precipitation method. In a typical preparation, copper nitrate ($Cu(NO_3)_2{\cdot}3H_2O$, 3.80 g), zirconyl nitrate ($ZrO(NO_3)_2{\cdot}xH_2O$, 2.54 g) and aluminium nitrate ($Al(NO_3)_3{\cdot}9H_2O$, 36.80 g) were dissolved in 500 mL of deionized water. The mixture was vigorous stirred at room temperature for 2 h. A 0.2 g/mL aqueous solution of potassium carbonate was added at a speed of 0.5 mL/min to the solution until the pH was 9.0. The precipitate was aged at room temperature for 48 h, filtered off, and washed thoroughly with deionized water until the effluent was neutral. The precipitate was dried at 100 ℃ for 24 h and calcined at 400 ℃ in stationary air for 4 h. Then, the catalyst was ground and pressed at 10 MPa to form pellets. The pellets were sieved to retain particles with sizes comprised 20 to 40 mesh. Prior to the reaction, the catalyst was reduced in flowing H_2 (100 mL/min) at 400 ℃ for 2 h. The calcined and reduced catalysts were labelled in the form *x*ZrCu-Al_2O_3, where *x* indicated the nominal weight percentage of zirconium on the Al_2O_3 support. In all catalysts, the nominal weight loading of copper on the Al_2O_3 support was fixed at 20 wt.%. For example, 10ZrCu-Al_2O_3 refers to the catalyst with 20% mass fraction of copper and 10% mass fraction of zirconium on the Al_2O_3 support. The catalysts with different zirconium mass fraction were also prepared as per the above-mentioned procedure.

2.3. Catalyst characterization

The BET surface area (S_{BET}) and pore volume (V_p) of the catalysts were measured by N_2 adsorption-desorption method at liquid nitrogen using Beishide instrument (3H-2000PS1). Prior to the measurement, the sample was degassed under vacuum at 200 ℃ for 12 h. The BET surface area was obtained as per the desorption branch of the isotherms.

Inductive coupled plasma optical emission spectroscopy (Optima 7300 DV, PerkinElmer) was used to measure the Cu content of the prepared catalysts and the chemical composition of the liquid product.

The X-ray diffraction (XRD) patterns were determined with a D2/max-RA X-ray diffractometer (Bruker, Germany) operating with Cu Kα radiation at 40 kV and 30 mA with a scanning angle (2ϑ) ranging from 10° to 90° at the scanning rate of 6°/min. The particle size was calculated using the Debye-Scherrer equation.

The reduction behaviors of the calcined catalysts were evaluated by H_2 temperature-programmed reduction (TPR) technique. Typically, the sample (50 mg) was loaded and pretreated in flowing He (30 mL/min) for 1 h at 400 ℃, followed by cooling at room temperature. After pretreatment, the reduction agent of a 5% H_2/N_2 flow (30 mL/min) was introduced. Then, the sample was heated to 700 ℃ at a rate of 10 ℃/min. The outlet gas was collected by passing it through a silica gel trap to remove water. The consumption of hydrogen was detected by a thermal conductivity detector.

The Cu dispersion and specific surface area (S_{Cu}) in the catalysts were measured by the dissociative N_2O chemisorption. Typically, the sample (50 mg) was pretreated in flowing He (30 mL/min) for 1 h at 400 ℃, followed by cooling at room temperature. The sample was reduced by increasing the temperature to 400 ℃ at a rate of 10 ℃/min with the reduction agent of a 5% H_2/N_2 flow (30 mL/min). Subsequently, the sample was exposed to N_2O flow (30 mL/min) for 0.5 h at 50 ℃ to oxidize the surface Cu^0 to Cu_2O. Next, TPR was carried out to reduce the Cu_2O to Cu by raising the temperature to 400 ℃ with the reduction agent of a 5% H_2/N_2 flow (30 mL/min).

The acidities of the catalysts were determined by ammonia temperature-programmed desorption (TPD) technique. Prior to the adsorption of NH_3, the sample (100 mg) was pretreated in flowing He (30 mL/min) for 1 h at 400 ℃ to remove moisture and other adsorbed gases. After cooling to 100 ℃, the sample was saturated with pure NH_3 for 0.5 h and subsequently purged with He (30 mL/min) for 1 h to remove the physically adsorbed NH_3. Next, the sample was heated to 750 ℃ at a rate of 10 ℃/min and the NH_3 desorption was monitored by a thermal conductivity detector.

X-ray photoelectron spectroscopy (XPS) analysis was performed on the Thermo Scientific™ ESCALAB™ 250Xi X-ray Photoelectron Spectrometer with Mg Kα radiation source (1253.6 eV) at a pressure of 3.0×10^{-7} mbar. The collected binding energies were corrected by the C1s peak at 284.6 eV as the reference. The binding energies were determined within a precision of ±0.1 eV.

The transmission electron microscope (TEM) images of the catalysts were obtained with FEI Tecnai G2 electron microscope operating at a 200 kV voltage. The sample was suspended in ethanol with an ultrasonic dispersion for 0.5 h. Drops of the suspension were deposited on copper grid coated with amorphous carbon film.

The SDT-Q600 thermogravimetric analysis (TGA) instrument was used for the characterization of the spent catalysts. A small quantity of the sample (200 mg) was placed in an aluminium sample cup and the temperature was increased from 50 ℃ to 900 ℃ at a rate of 10 ℃/min in air atmosphere.

2.4. Catalytic activity test

The glycerol hydrogenolysis was carried out in a vertical fixed-bed reactor with a back pressure regulator to control the system pressure. The reactor was stainless steel tube with an internal diameter of 11 mm and a length of 950 mm. A schematic diagram of the experimental apparatus is displayed in Figure S1. In a typical run, 4.0 g catalyst (20-40 mesh, *ca.* 5 mL) was charged in the constant temperature section of the reactor tube, with quartz sand packed in both ends. Before the catalytic activity test, the catalyst

was *in situ* reduced in pure H_2 with a flow rate of 100 mL/min at 400 ℃ for 2 h. After reduction, the temperature of the reactor was decreased to 230 ℃ and pressured to 3.5 MPa. A 20 wt.% glycerol ethanol (or water, methanol, 1-propanol) solution was continuously fed into the reactor with a flow rate of 27.8 mL/h, which corresponded to WHSV ((weight flow rate of the feed solution)×(weight fraction of glycerol in the feed)/(weight of the catalyst)) of 1.21 h^{-1}, in pure H_2 (or N_2) flow at 100 mL/min (mole ratio of H_2:glycerol = 95:1). The reaction products were cooled in a condenser and collected in a gas-liquid separator. The liquid samples were withdrawn at regular intervals of time (0.5 h). The collected liquid samples were analyzed by a gas chromatography (Shimadzu GC-2014), equipped with a flame ionization detector and a capillary column (Rtx-WAX, 30 m × 0.25 mm). 1,4-Butanediol was added to the liquid sample as an internal standard substance for the GC analysis. The steady state performance of the reactor was observed by GC analysis of the liquid samples after reaction for 2 h and data acquisition was carried out after steady operation for 3 h. The obtained results were averages of 3-4 data points at the same conditions. Each data point was analyzed three times by GC. The mass balances were greater than 95% for each set of data acquisition. The liquid products were also identified by GC-MS (Shimadzu GCMS-QP2010). The conversion of glycerol and selectivity of products were defined as follows. The standard uncertainties of the conversion and selectivity in the samples were 1%.

$$\text{Conversion}(\%)=\frac{\text{moles of glycerol(in)}-\text{moles of glycerol(out)}}{\text{moles of glycerol(in)}}\times 100$$

$$\text{Selectivity}\,(\%)=\frac{\text{moles of carbon in a specific product}}{\text{moles of carbon in glycerol consumed}}\times 100$$

$$\text{Yield}\,(\%)=\frac{\text{Conversion}\,(\%)\times\text{Selectivity}\,(\%)}{100}$$

3. Results and discussion

3.1. Catalyst Characterization

3.1.1. Physicochemical properties of the catalysts

The physicochemical properties of the catalysts are summarized in Table 1. Compared with Cu-Al_2O_3 catalyst, the ZrO_2-promoted Cu-Al_2O_3 catalysts had high BET surface area and pore volume. However, the incorporation of ZrO_2 into Cu-Al_2O_3 slightly reduced the weight loading of Cu and the pore size of the catalysts (Figure S2). On the other hand, addition of ZrO_2 to Cu-Al_2O_3 notably decreased Cu particle size and enhanced the Cu dispersion and specific surface area. These behaviours showed that the ZrO_2 contributed to restraining the aggregation of Cu particles during the thermal treatment, which might be due to the strong interaction between zirconium and copper species.[24,25] Similar behavior was also reported elsewhere for the ZrO_2-promoted Cu/ZnO/Cr_2O_3 catalysts.[23]

Table 1 Physicochemical property of the catalysts

Catalyst	S_{BET} (m^2g^{-1})	V_p (cm^3g^{-1})	Cu content (wt.%)[a]	d_{Cu} (nm)[b]	Cu dispersion (%)[c]	S_{Cu} (m^2g^{-1})[c]	d_{Cu} (nm)[c]	Acidity (μmol NH_3 g^{-1})[d]	Acidity 420-750 ℃ (μmol NH_3 g^{-1})[d]
Cu-Al_2O_3	64.2	0.236	17.6	19.4	7.8	52.8	12.8	627	444
5ZrCu-Al_2O_3	89.5	0.279	17.2	15.7	11.4	77.1	8.8	1436	1242
10ZrCu-Al_2O_3	103.4	0.302	16.9	9.8	15.0	101.5	6.7	1686	1487
20ZrCu-Al_2O_3	117.9	0.317	16.3	6.5	18.7	126.5	5.3	2175	1972
30ZrCu-Al_2O_3	100.1	0.295	15.1	5.9	17.3	117.0	5.8	2261	2121

[a] Measured from ICP. [b] Estimated from XRD. [c] Measured from N_2O chemisorption. [d] Measured from NH_3-TPD.

3.1.2. Structural properties of the catalysts

The XRD patterns of the catalysts after calcination at 400 ℃ for 4 h are presented in Figure 1 A. The presence of the peaks at 2ϑ = 32.5°, 35.5° and 38.7° corresponded to CuO (PDF#48-1548),[23] peaks at 2ϑ = 46.3° and 67.0° to Al_2O_3 (PDF#13-0373),[26] and peaks at 2ϑ = 23.9°, 29.5° and 33.9° to monoclinic ZrO_2.[25] With the increase in zirconium content, the intensity of diffraction peaks for monoclinic ZrO_2 increased remarkably. Interestingly, almost no peaks of CuO were observed on the ZrO_2-promoted Cu-Al_2O_3 catalysts, which was likely related to the decreased Cu loading and homogeneous distribution of CuO particles on the support surface. As shown in Figure 1 B, after reduction at 400 ℃ for 2 h, the diffraction peaks of monoclinic ZrO_2 and CuO disappeared, while the peaks of Cu (PDF#04-0836) were detected in the catalysts.[23] The diffraction peaks of Cu enlarged and their intensities notably decreased with an increase in zirconium content. The Cu particle size (given in Table 1) was remarkably decreased from 19.4 nm for Cu-Al_2O_3 to 5.9 nm for 30ZrCu-Al_2O_3. The results above indicated that the introduction of ZrO_2 could suppress the increase of Cu particles, which resulted in the increased Cu dispersion.

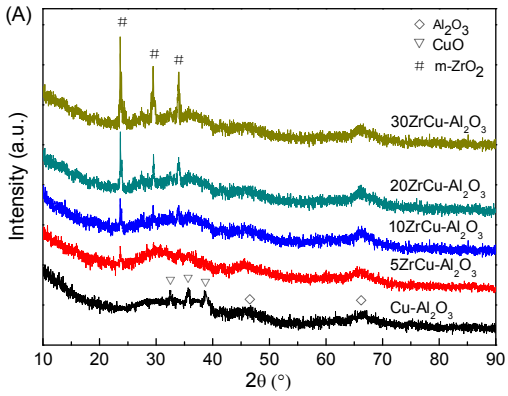

View Article Online
DOI: 10.1039/C6CY00085A

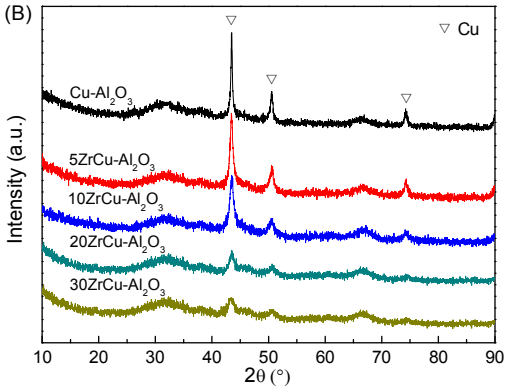

Figure 1. XRD patterns of the catalysts upon calcination (A); reduction (B).

3.1.3. Reducibility and surface acidic properties of the catalysts

The H_2-TPR profiles of the catalysts are displayed in Figure 2 A. In order to get a deeper understand about the results of H_2-TPR, the reduction peak can be classified into two sections, one at low temperature (peak *α*) and another at relatively high temperature (peak *β*). The low temperature peak *α* can be associated with the reduction of highly dispersed CuO with smaller particle size, while high temperature peak *β* can be ascribed to the reduction of bulk CuO with a larger size.[17] As can be seen, the Cu species in Cu-Al_2O_3 catalyst was mainly present in the form of bulk CuO. For the ZrO_2-promoted Cu-Al_2O_3 catalysts, the intensity of low temperature peak *α* increased significantly while that of high temperature peak *β* declined notably with the increase in zirconium content, suggesting addition of ZrO_2 to Cu-Al_2O_3 favored the formation of highly dispersed Cu species.

As shown in Figure 2 B, the acidity of the catalyst was measured by NH_3-TPD. Based on the temperature of NH_3 desorption peak, the acid sites of the catalyst can be divided into three sections, weak acid (150-250 ℃), medium acid (250-420 ℃), and strong acid (420-750 ℃) strength.[27,28] As can be seen from Figure 2 B, almost no NH_3 desorption peak was observed on Al_2O_3 support. The Cu-Al_2O_3 catalyst showed a broad peak of NH_3 desorption at 150-350 ℃, implying the presence of weak and medium acid sites, while small amounts of strong acid sites were evident from another broad peak at 420-750 ℃. In the case of ZrO_2-promoted Cu-Al_2O_3 catalysts, a strong NH_3 desorption peak in the temperature range of 450-750 ℃ was observed, indicating the existence of large amounts of strong acid sites. To illustrate, the acidities of catalysts are listed in Table 1. It can be observed from Table 1 that incorporation of ZrO_2 into Cu-Al_2O_3 catalyst not only enhanced the acid quantity, but also increased the strong acid sites, which might be related to the strong acid nature of ZrO_2.[29,30] Moreover, it should be pointed out that the NH_3 desorption peak centred at *ca.* 630 ℃ for the ZrO_2-promoted Cu-Al_2O_3 catalysts slightly moved to higher temperature with the increase in zirconium content, confirming the higher the zirconium content the higher the acid strength.

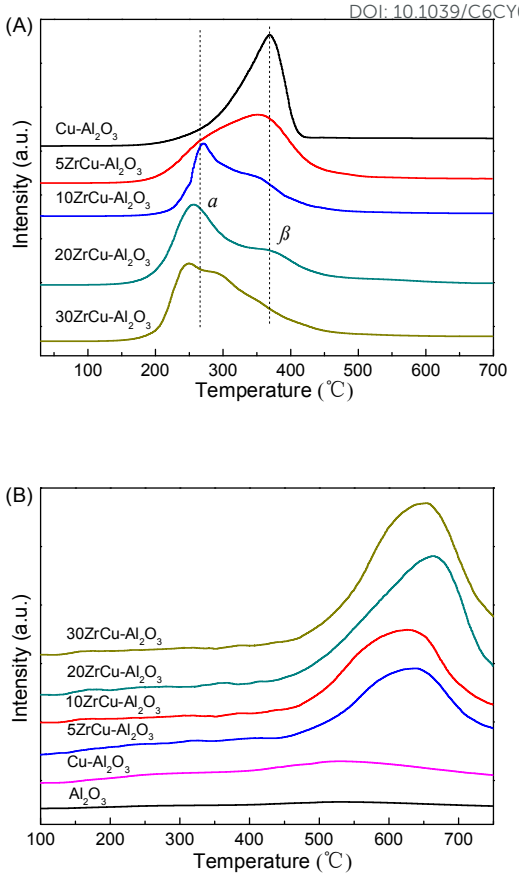

Figure 2. H_2-TPR (A) and NH_3-TPD (B) profiles of the catalysts.

3.1.4. Surface element compositions of the catalysts

The surface element compositions of catalysts were analyzed using XPS technique. Figure 3 displays the Cu 2p and Zr 3d XPS spectra of the catalysts and the binding energy (B.E.) values of Cu, Zr, Al and O are given in Table S1. As shown in Figure 3 A, the calcined catalysts showed the B.E. values of about 934.5 and 954.5 eV respectively corresponding to Cu $2p_{3/2}$ and Cu $2p_{1/2}$. Meanwhile, the main peaks were followed by two strong satellite peaks at *ca.* 943 and 963 eV, implying the presence of Cu^{2+} species in the catalysts.[16,31] After reduction at 400 ℃ for 2 h, the two peaks (Figure 3 B) at *ca.* 932.5 and 952.5 eV on XPS spectra for the catalysts were respectively ascribed to Cu $2p_{3/2}$ and Cu $2p_{1/2}$ of Cu^0.[17] The low B.E. values and absence of satellite peaks showed that the Cu^{2+} species in the catalysts were fully reduced to Cu^0.[8] Furthermore, the two peaks (Figure 3 C) at *ca.* 182.0 and 184.5 eV for the catalysts were attributed to Zr $3d_{5/2}$ and Zr $3d_{3/2}$ peaks of Zr^{4+}, respectively.[24] As can be seen from Table S1, the catalysts showed the B.E. values of about 73 and 74 eV respectively ascribed to Al $2p_{3/2}$ and Al $2p_{1/2}$, confirming the existence of Al^{3+} species. The O 1s spectra for the catalysts exhibited two peaks at *ca.* 531 and 533 eV. The peak at *ca.* 531 eV was ascribed to the lattice oxygen, while the peak at *ca.* 533 eV could be related to the presence of hydroxyl species.[10] Interestingly, the Cu 2p peaks (Figure 3 B) for the catalysts slightly shifted to higher B.E. when adding of ZrO_2 to Cu-Al_2O_3, while the Zr 3d spectra (Figure 3 C) moved to lower B.E., showing the existence of charge transfer from the copper metal

ions to the ZrO_2 and/or Al_2O_3 species. This behaviour was probably due to the strong interaction between the CuO and ZrO_2 and/or Al_2O_3 species. Similar behaviours were also presented in elsewhere.[17,24,31] In addition, it's also worth noting that in spite of almost the same Cu loading, the introduction of ZrO_2 into Cu-Al_2O_3 notably increased the surface Cu/Al atomic ratio (Table S1), which showed the addition of ZrO_2 was beneficial to improve the Cu dispersion.

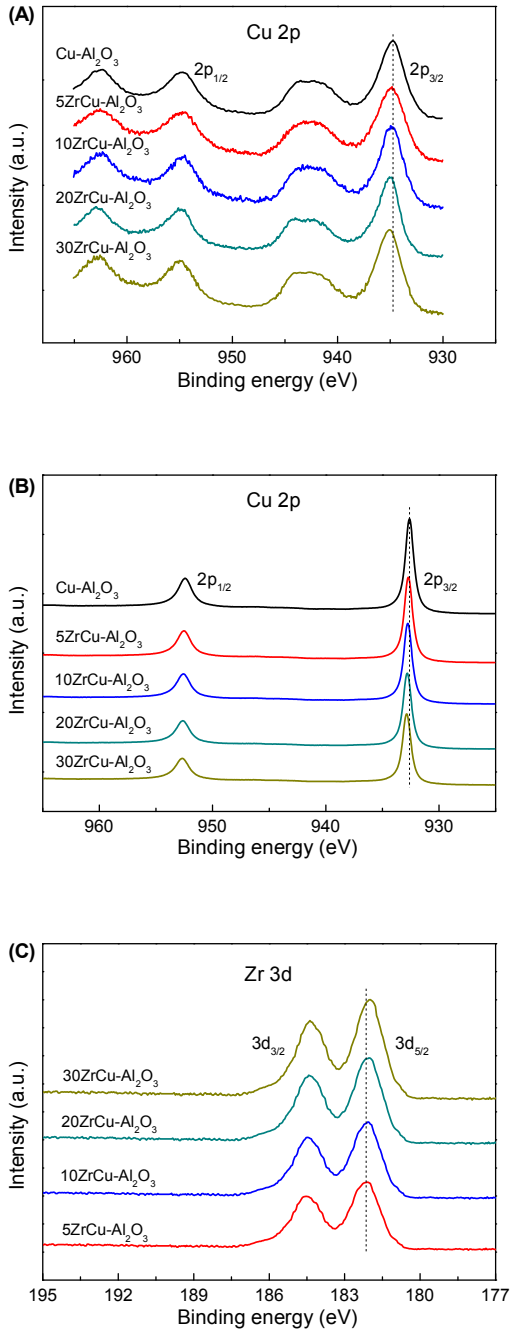

Figure 3. Cu 2p XPS profiles of calcined (A) and reduced (B) catalysts, Zr 3d XPS profiles of reduced catalysts (C).

3.2. Glycerol hydrogenolysis studies

3.2.1. Catalytic activity

The catalytic activity of the catalyst was studied in a fixed-bed reactor at 230 ℃ and 3.5 MPa using ethanol as a solvent. For the purpose of comparison, catalytic activity of alumina prepared by precipitation method is also listed in Table 2. As can be seen, very low glycerol conversion and 1,2-PDO selectivity were obtained on alumina. In the case of Cu-Al_2O_3 catalyst, the glycerol conversion and 1,2-PDO selectivity respectively were 64.9% and 82.7%. The glycerol conversion and 1,2-PDO selectivity notably increased when ZrO_2 was added to Cu-Al_2O_3. Among the catalysts tested, the 20ZrCu-Al_2O_3 catalyst obtained the excellent catalytic performance with 97.1% glycerol conversion and 95.3% 1,2-PDO selectivity. This result was much better than that attained by other Cu-based catalysts.[32–34] Nevertheless, further increase in zirconium content led to slight decrease of 1,2-PDO selectivity, which might be due to the reduction of Cu dispersion in the catalyst, as confirmed by N_2O chemisorption. On the other side, addition of ZrO_2 to Cu-Al_2O_3 decreased the selectivities to ethylene glycol and acetol, suggesting that the C-C bond breaking reaction for glycerol was restrained to some extent and the introduction of ZrO_2 contributed to the hydrogenation of acetol. The results above obviously showed the high catalytic performance of ZrO_2-promoted Cu-Al_2O_3 catalysts.

Table 2 Catalytic results of glycerol hydrogenolysis on different catalysts[a]

Catalyst	Conversion (%)	Selectivity (%)[b]			
		1,2-PDO	EG	Acetol	Others
Al_2O_3	1.2	0.2	Trace	98.3	1.5
Cu-Al_2O_3	64.9	82.7	4.8	4.2	8.3
5ZrCu-Al_2O_3	80.2	85.9	3.7	2.6	7.8
10ZrCu-Al_2O_3	86.4	92.6	2.4	0.9	4.1
20ZrCu-Al_2O_3	97.1	95.3	1.2	0.3	3.2
30ZrCu-Al_2O_3	98.5	92.0	1.9	1.4	4.7

[a] Reaction conditions: 20 wt.% glycerol ethanol solution; liquid flow rate, 27.8 mL/h; hydrogen flow rate, 100 mL/min; H_2:glycerol = 95:1 (mole ratio); catalyst weight, 4.0 g (*ca.* 5 mL); WHSV = 1.21 h^{-1}; reaction temperature, 230 ℃; operating pressure, 3.5 MPa; data acquisition after steady operation for 3 h. [b] 1,2-PDO = 1,2-propanediol; EG = ethylene glycol; others include methanol, 1-propanol, 2-propanol, 1,3-propanediol, etc.

It has been well established that the acid-catalyzed hydrogenolysis of glycerol proceeds by the C-O bond scission step that involves the dehydration of glycerol molecules to produce acetol on acid sites of support, and followed by hydrogenation of acetol to produce 1,2-PDO on metal active sites of catalyst.[17–19,28,35] Thereby, the amounts of acid and metal active sites in the catalyst have great effects on the hydrogenolysis of glycerol to 1,2-PDO. As shown in Figure 4 A, very low glycerol conversion and 1,2-PDO selectivity were achieved on alumina, most probably due to the lack of acid and metal active sites on alumina surface. Conversely, the catalytic activity increased significantly for the Cu-Al_2O_3 catalyst (Figure 4 B) due to the presence of acid and Cu active sites . However, because the Cu-Al_2O_3 catalyst was very low in acid, as proved by NH_3-TPD, only 64.9% glycerol conversion was obtained. As ZrO_2 was introduced into Cu-Al_2O_3 catalyst, the acidity and Cu dispersion were enhanced notably, which resulted in the improved catalytic performance for glycerol hydrogenolysis (Figure 4 C).

Journal Name

View Article Online
DOI: 10.1039/C6CY00085A

ARTICLE

Figure 4. Proposed reaction pathway for glycerol hydrogenolysis in Al_2O_3 (A), Cu-Al_2O_3 (B) and 20ZrCu-Al_2O_3 (C).

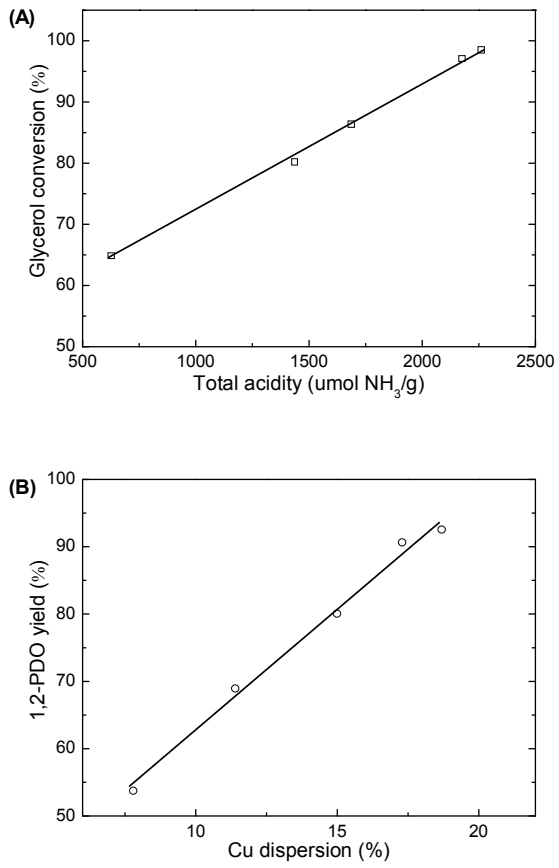

Figure 5. Variation of glycerol conversion with total acidity in the catalysts (A) and 1,2-PDO yield as a function of Cu dispersion for the catalysts (B). Reaction conditions: 20 wt.% glycerol ethanol solution; liquid flow rate, 27.8 mL/h; hydrogen flow rate, 100 mL/min; H_2:glycerol = 95:1 (mole ratio); catalyst weight, 4.0 g (*ca.* 5 mL); WHSV = 1.21 h^{-1}; reaction temperature, 230 ℃; operating pressure, 3.5 MPa; data acquisition after steady operation for 3 h.

As stated above, it has been reported that the hydrogenolysis of glycerol was strongly influenced by the acidity of the catalysts.[31,36–38] Also, the role of acid and metal active sites on glycerol hydrogenolysis has been investigated by different researchers.[17–19,39] Their results indicated that more acid and metal active sites in the catalysts favored the increased catalytic performance for glycerol hydrogenolysis. To get a deeper understand about the nature of active species in the hydrogenolysis of glycerol to 1,2-PDO on the ZrO_2-promoted Cu-Al_2O_3 catalysts, we attempted to explore the relationship between structural properties of catalysts and catalytic performance for glycerol hydrogenolysis. As shown in Figure 5 A, a clear correlation between glycerol conversion and total acidity was observed. Glycerol conversion increased with increasing total acidity of the catalyst. Numerous studies have suggested that the acid-catalyzed hydrogenolysis of glycerol was first dehydrated to acetol at Lewis acid sites or 3-hydroxypropanal at Bronsted acid sites, which were subsequently hydrogenated to 1,2- and 1,3-PDO, respectively.[19,37] Hence, the acidity of the ZrO_2-promoted Cu-Al_2O_3 catalysts might be mainly composed of Lewis acid because a very low level of 1,3-PDO and high concentrations of 1,2-PDO were detected in this work. Nevertheless, it should be noted that the presence of the Cu active sites was necessary to the hydrogenolysis of glycerol to 1,2-PDO.[17,18] A closely linear correlation between 1,2-PDO yield and Cu dispersion was presented in Figure 5 B, showing that the Cu active sites on the support surface were mainly responsible for the hydrogenation of acetol to 1,2-PDO. Therefore, introduction of ZrO_2 into Cu-Al_2O_3 not only improved 1,2-PDO selectivity but also decreased the selectivity to acetol. The excessive acetol on Cu-Al_2O_3 catalyst can be transformed into 1,2-PDO due to the presence of more available Cu active sites on ZrO_2-promoted Cu-Al_2O_3 catalysts. In short, the results in this work demonstrated that both acid sites and Cu active sites in the catalysts were the key parameters for the efficient hydrogenolysis of glycerol to 1,2-PDO.

3.2.2. Effect of solvent

It's well known that the glycerol can be generated as a by-product in the manufacture of biodiesel and is presented in water phase. And water is a by-product of the glycerol hydrogenolysis. Therefore, water seems to be the most suitable solvent for the hydrogenolysis of glycerol to 1,2-PDO in view of environment protection and economic benefits. On the other side, different alcohols have been widely used as the solvents and/or hydrogen donors for the hydrogenolysis of glycerol.[32–34,40–44] Typically, methanol and 1-propanol were used for studying the effect of solvent on glycerol hydrogenolysis over 20ZrCu-Al_2O_3 catalyst. As displayed in Figure 6, the catalytic activity of the catalyst was strongly affected by the selection of solvent. The maximum (97.1%) and minimum (56.4%) glycerol conversion respectively were

achieved when ethanol and water were selected as solvents. In addition, in the case of 1-propanol as a solvent, glycerol conversion and 1,2-PDO selectivity were 94.6% and 92.4%, respectively, slightly greater than those in the presence of methanol as a solvent.

Vasiliadou et al[33] suggested that there was a linear relationship between the glycerol conversion and hydrogen concentration in the solution when 1-butanol was used as a solvent for the hydrogenolysis of glycerol. Thereby, the concentration of hydrogen was supposed to be a key factor in glycerol conversion. In this work, the glycerol conversion in different solvents decreased in the order of ethanol > 1-propanol > methanol > water, which was in agreement with the results of the solubility of hydrogen in the corresponding solvents.[45,46] On the other hand, because the alcohols such as methanol, ethanol, 1-propanol, 2-propanol, and 1-butanol were considered to be the appropriate hydrogen donors for glycerol hydrogenolysis, the catalytic hydrogen transformation from alcohols to glycerol also favored the improved glycerol conversion compared to water as a solvent.[11,40–44] To further understand the effect of solvent on glycerol hydrogenolysis, different alcohols (methanol, ethanol and 1-propanol) were used as hydrogen donors for the hydrogenolysis of glycerol. Table 3 summarizes the catalytic performance for glycerol hydrogenolysis in different hydrogen donors. As can be seen, the best catalytic performance (19.7% glycerol conversion and 30.4% 1,2-PDO selectivity) was achieved when ethanol was adopted as a hydrogen donor, but the selectivity to acetol was very high (59.6%), suggesting the lack of available hydrogen for the hydrogenation of acetol to 1,2-PDO. The glycerol conversion and 1,2-PDO selectivity respectively were 17.2% and 28.6% when using 1-propanol as a hydrogen donor, greater than those in the case of methanol as a hydrogen donor. The glycerol conversion for different hydrogen donors followed this order: ethanol > 1-propanol > methanol, consistent well with the literature reports.[41] In sum, the results above clearly demonstrated that ethanol was the most effective hydrogen donor, which could be another reason for the high catalytic activity when glycerol hydrogenolysis was performed in ethanol solution.

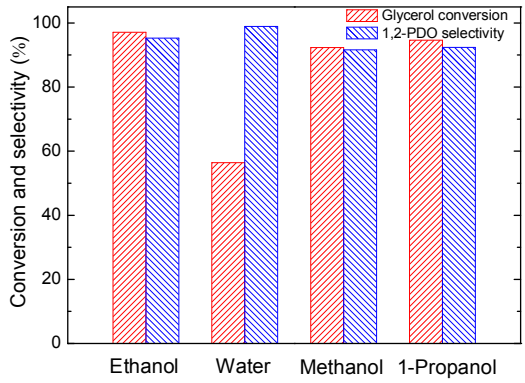

Figure 6. Effect of solvent on glycerol hydrogenolysis over 20ZrCu-Al_2O_3 catalyst. Reaction conditions: 20 wt.% glycerol concentration; liquid flow rate, 27.8 mL/h; hydrogen flow rate, 100 mL/min; H_2:glycerol = 95:1 (mole ratio); catalyst weight, 4.0 g (*ca.* 5 mL); reaction temperature, 230 ℃; operating pressure, 3.5 MPa; data acquisition after steady operation for 3 h.

Table 3 Different hydrogen donors for glycerol hydrogenolysis on 20ZrCu-Al_2O_3 catalyst[a]

Solvent	Conversion (%)	Selectivity (%)[b]			
		1,2-PDO	EG	Acetol	Others
Methanol	13.1	24.9	0.6	65.3	9.2
Ethanol	19.7	30.4	1.1	59.6	8.9
1-Propanol	17.2	28.6	0.8	62.1	8.5

[a] Reaction conditions: 20 wt.% glycerol concentration; liquid flow rate, 27.8 mL/h; nitrogen flow rate, 100 mL/min; catalyst weight, 4.0 g (*ca.* 5 mL); reaction temperature, 230 ℃; operating pressure, 3.5 MPa; data acquisition after steady operation for 3 h. [b] 1,2-PDO = 1,2-propanediol; EG = ethylene glycol; others include methanol, ethanol, formaldehyde, acetaldehyde, propionaldehyde, 1-propanol, 2-propanol, etc.

It should be emphasized, however, that 98.9% 1,2-PDO selectivity was achieved in the presence of water as a solvent, as shown in Figure 6. In comparison to the alcohols like methanol, ethanol, and 1-propanol, the water had the higher polarity and proton transfer ability so that the target product 1,2-PDO could more easily migrate from the catalytic surface in an aqueous solution, which resulted in the high selectivity to 1,2-PDO.[43,47] Conversely, the polarities of alcohols were weaker with lower proton transfer ability, which led to the formation of more by-products. But any way, the best catalytic performance was achieved in the case of ethanol as a solvent. Therefore, further experiments were performed on 20ZrCu-Al_2O_3 catalyst using ethanol as a solvent.

3.2.3. Effect of reaction temperature

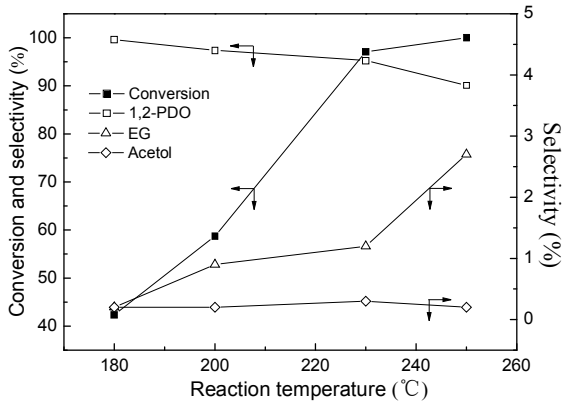

Figure 7. Effect of reaction temperature on glycerol hydrogenolysis over 20ZrCu-Al_2O_3 catalyst. Reaction conditions: 20 wt.% glycerol ethanol solution; liquid flow rate, 27.8 mL/h; hydrogen flow rate, 100 mL/min; catalyst weight, 4.0 g (*ca.* 5 mL); WHSV = 1.21 h^{-1}; operating pressure, 3.5 MPa; data acquisition after steady operation for 3 h.

The effect of reaction temperature on glycerol hydrogenolysis was investigated in the range of 180 to 250 ℃ on 20ZrCu-Al_2O_3 catalyst. As displayed in Figure 7, the glycerol conversion rapidly enhanced from 42.4 to 100% when the reaction temperature was increased from 180 to 250 ℃. Nevertheless, the selectivity to 1,2-PDO was found to be slightly declined with the increase of reaction temperature. It should be noted that the selectivity to acetol was very low in the full temperature range (180-250 ℃), indicating the

View Article Online
DOI: 10.1039/C6CY00085A

high efficiency of 20ZrCu-Al_2O_3 catalyst for glycerol hydrogenolysis. Conversely, the selectivity to ethylene glycol increased marginally from 0.2 to 2.7%. The improvement in selectivity of ethylene glycol was likely related to the fact that the hydrogenolysis of 1,2-PDO to ethylene glycol might occur on Cu active sites of the catalyst at high reaction temperature.[32] In addition, the high reaction temperature also favored direct hydrogenolysis of glycerol to ethylene glycol.[9] Thus, an appropriate reaction temperature was necessary for the hydrogenolysis of glycerol to 1,2-PDO. The temperature of 230 ℃ was selected to further study.

3.2.4. Effect of operating pressure

The glycerol hydrogenolysis was performed at different operating pressures to assess the catalytic activity of the 20ZrCu-Al_2O_3 catalyst. As shown in Figure 8, the glycerol conversion was remarkable increased from 89.4 (2.5 MPa) to 100% (4 MPa) and then remained at 100% with the increase in the operating pressure. As the solubility of hydrogen in ethanol solution was raised with the improvement of operating pressure,[45] more hydrogen molecules were available to be absorbed on catalytic surface, which led to the increase of glycerol conversion. Meanwhile, the improvement of operating pressure also favored the sequential hydrogenolysis of glycerol to 1,2-PDO. Nevertheless, the selectivity to acetol notably declined with the increase of operating pressure. The lack of available hydrogen molecules at low operating pressure might lead to significant accumulation of acetol. Conversely, hydrogen molecules could more easily reach the Cu active sites of the catalyst at high operating pressure, which resulted in the rate of acetol hydrogenation to 1,2-PDO exceed by far its formation rate via glycerol dehydration.[33] For this reason, it was understood that the selectivity to acetol decreased with the increase in operating pressure. In general, glycerol hydrogenolysis at low operating pressure was the key to reduce the equipment cost and ensure an economic operation. Thus, the hydrogen pressure of 3.5 MPa was supposed to be the optimum value in consideration of the catalytic activity and economic interest.

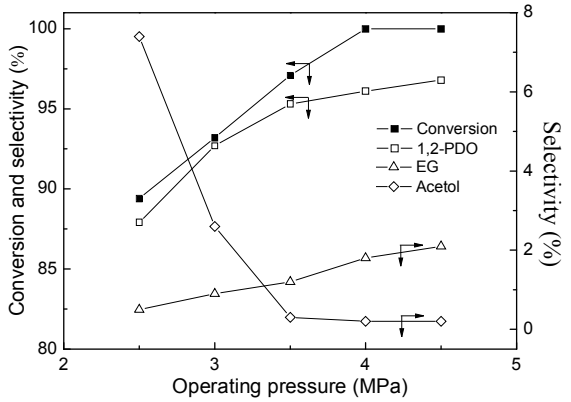

Figure 8. Effect of operating pressure on glycerol hydrogenolysis over 20ZrCu-Al_2O_3 catalyst. Reaction conditions: 20 wt.% glycerol ethanol solution; liquid flow rate, 27.8 mL/h; hydrogen flow rate, 100 mL/min; catalyst weight, 4.0 g (*ca.* 5 mL); WHSV = 1.21 h^{-1}; reaction temperature, 230 ℃; data acquisition after steady operation for 3 h.

3.2.5. Effect of glycerol concentration

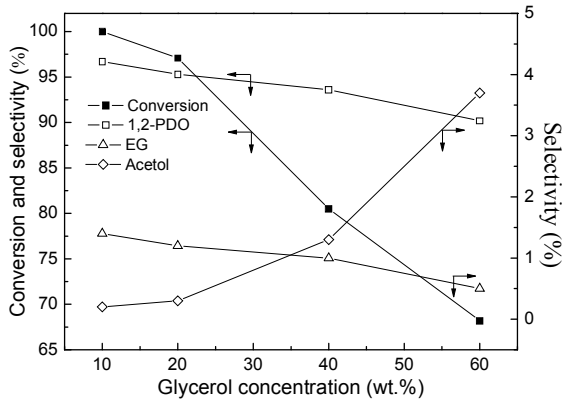

Figure 9. Effect of glycerol concentration on glycerol hydrogenolysis over 20ZrCu-Al_2O_3 catalyst. Reaction conditions: solvent, ethanol; liquid flow rate, 27.8 mL/h; hydrogen flow rate, 100 mL/min; catalyst weight, 4.0 g (*ca.* 5 mL); reaction temperature, 230 ℃; operating pressure, 3.5 MPa; data acquisition after steady operation for 3 h.

To obtain maximum productivity of 1,2-PDO, different glycerol concentrations were selected for studying the catalytic performance for glycerol hydrogenolysis. It can be observed from Figure 9 that the glycerol conversion was rapidly decreased from 100 to 68.2% when the glycerol concentration was increased from 10 to 60 wt.%. The reasons for this behaviour might be associated with the two factors: (1) when the glycerol concentration was raised, the increase in the viscosity of the solution would lead to more external mass transfer limitations,[33] which was not beneficial to the glycerol hydrogenolysis; (2) as the quantity of catalyst was maintained constant, the growing number of glycerol molecules resulted in the reduction in catalyst to glycerol ratio, and consequently less number of Cu active sites was available to the hydrogenolysis of glycerol. Similarly, the selectivity to 1,2-PDO slightly decreased from 96.7 to 90.2% with the increase of glycerol concentration from 10 to 60 wt.%. As the glycerol concentration was increased, the large amounts of glycerol molecules were presented in the feedstock, which would lead to the reduction of the solubility of hydrogen in solution.[33] Thus, the selectivity to 1,2-PDO was diminished slightly while the selectivity to acetol enhanced slowly with the increase in glycerol concentration. In addition, very low ethylene glycol (< 2%) was detected within the whole range of glycerol concentration (10-60wt.%), suggesting the high selectivity of the 20ZrCu-Al_2O_3 catalyst.

3.2.6. Effect of liquid flow rate

In order to enhance the efficiency of glycerol hydrogenolysis, the effect of liquid flow rate on glycerol hydrogenolysis was tested in the range of 13.2 to 88.8 mL/h on 20ZrCu-Al_2O_3 catalyst. As shown in Figure 10, the glycerol conversion was significantly dropped with the increase in liquid flow rate. The reason for the reduction in glycerol conversion might be attributed to the decrease in residence time of glycerol on the catalytic surface when the liquid flow rate was increased. On the other side, the catalyst particles were partially wetted at a low liquid flow rate. The hydrogen

molecules could more easily to get intimate contact with glycerol molecules on catalytic surface because of the less external mass transfer limitations. Subsequently at a high liquid flow rate, the increase in wetted fractions of catalytic surface would lead to the reduction of the reaction rate.[32] Similarly, the selectivity to 1,2-PDO was found to be decreased from 96.2 to 75.1%, while the selectivity to acetol enhanced dramatically from 0.2 to 16.4% when the liquid flow rate was increased from 13.2 to 88.8 mL/h. The less residence time at high liquid flow resulted in the lack of the intimate contact between the hydrogen molecules and glycerol molecules on the catalytic surface. Therefore, the selectivity to acetol increased at the expense of 1,2-PDO with the increase in liquid flow rate.

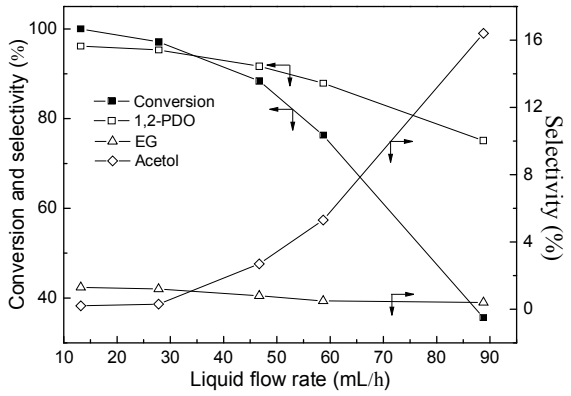

Figure 10. Effect of liquid flow rate on glycerol hydrogenolysis over 20ZrCu-Al_2O_3 catalyst. Reaction conditions: 20 wt.% glycerol ethanol solution; hydrogen flow rate, 100 mL/min; catalyst weight, 4.0 g (*ca.* 5 mL); reaction temperature, 230 ℃; operating pressure, 3.5 MPa; data acquisition after steady operation for 3 h.

3.2.7. Stability test

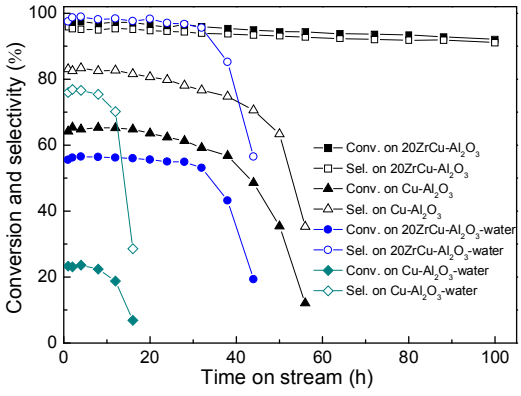

Figure 11. The stability test of the catalyst. Reaction conditions: 20 wt.% glycerol ethanol (or water) solution; liquid flow rate, 27.8 mL/h; hydrogen flow rate, 100 mL/min; H_2:glycerol = 95:1 (mole ratio); catalyst weight, 4.0 g (*ca.* 5 mL); reaction temperature, 230 ℃; operating pressure, 3.5 MPa.

As stability is essential to the practical application of catalyst, the stability of 20ZrCu-Al_2O_3 catalyst has been tested in this work. In addition, the stability of Cu-Al_2O_3 catalyst was also investigated as a reference in different solvents. As displayed in Figure 11, the glycerol conversion and 1,2-PDO selectivity were slowly decreased, but their values were still higher than 90% after 100 h time on stream on 20ZrCu-Al_2O_3 catalyst in the presence of ethanol as a solvent. Conversely, serious deactivation was observed on Cu-Al_2O_3 catalyst after 56 h continuous operation when ethanol was selected as a solvent. Moreover, the Cu-Al_2O_3 catalyst exhibited the loss of catalytic activity after only 16 h in the case of water as a solvent. By contrast, the catalytic activity of 20ZrCu-Al_2O_3 was relatively stable for 30 h under the same reaction conditions. But the further extension of reaction time, the deactivation of catalyst was also observed. But anyway, the results of the stability test indicated that the ZrO_2-promoted Cu-Al_2O_3 catalyst had a better stability and prospective for practical application compared to Cu-Al_2O_3 catalyst.

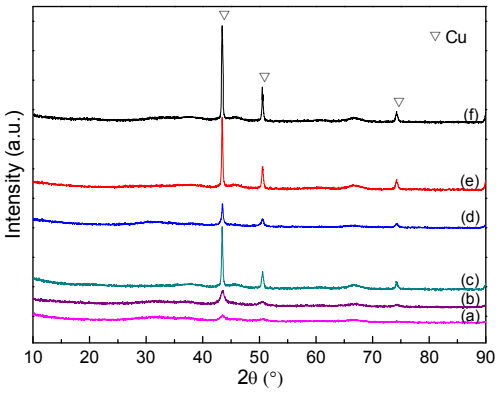

Figure 12. XRD patterns of the catalysts: (a) fresh 20ZrCu-Al_2O_3; (b) spent 20ZrCu-Al_2O_3 using ethanol as a solvent; (c) spent 20ZrCu-Al_2O_3 using water as a solvent; (d) fresh Cu-Al_2O_3; (e) spent Cu-Al_2O_3 using ethanol as a solvent; (f) spent Cu-Al_2O_3 using water as a solvent.

The deactivation of Cu-based catalysts has been widely reported in the literature so far. Some researchers[12,17,44] suggested that the sintering of Cu particles was mainly responsible for the loss of catalytic activity in the presence of water as a solvent, while other studies[34,48] showed the reason of deactivation was related to Cu particles sintering and the presence of adsorbed species on the catalytic surface. In order to clarify the reason of catalyst deactivation in this work, the spent catalyst was submitted to several characterization techniques. First, inductive coupled plasma optical emission spectroscopy (ICP-OES) was used to measure the chemical composition of the liquid product. The deactivation of catalyst cannot be assigned to metal leaching, because the results of ICP-OES analysis showed negligible copper, zirconium and aluminium contents in the liquid product. Secondly, the BET surface area measurement of the spent catalysts was carried out. The BET surface area of the spent catalysts slightly decreased (Cu-Al_2O_3 = 48.7 m^2g^{-1} and 20ZrCu-Al_2O_3 = 101.0 m^2g^{-1}) when ethanol was selected as a solvent. In comparison to ethanol as a solvent, the use of water as a solvent resulted in a significant reduction in the BET surface area of the spent catalysts (Cu-Al_2O_3 = 25.8 m^2g^{-1} and 20ZrCu-Al_2O_3 = 86.3 m^2g^{-1}). The decrease in BET surface area might be related to the collapse of the alumina support and/or partial pore blockage. Furthermore, the XRD determination was performed to observe the structure change of the spent catalyst. As shown in

View Article Online
DOI: 10.1039/C6CY00085A

Figure 12, the Cu particle size of spent 20ZrCu-Al_2O_3 catalyst slowly increased from 6.5 to 13.9 nm after 100 h continuous operation in the case of ethanol as a solvent. In contrast, the Cu particle size of spent Cu-Al_2O_3 catalyst after only 56 h time on stream dramatically increased from 19.4 to 31.7 nm when ethanol was adopted as a solvent. Moreover, the Cu particle size with 44.6 nm was presented on spent Cu-Al_2O_3 catalyst after 16 h reaction time when using water as a solvent. However, the Cu particle size of spent 20ZrCu-Al_2O_3 catalyst moderately increased from 6.5 to 28.3 nm despite with a longer reaction time (44 h) in the presence of water as a solvent. The results of XRD analysis obviously showed that the sintering of Cu particles was the key factor for the loss of catalytic activity. The spent catalyst was also characterized by TEM. As displayed in Figure 13, some obvious agglomerates were observed on spent Cu-Al_2O_3 catalyst after 56 h continues operation in the case of ethanol as a solvent. Moreover, the spent Cu-Al_2O_3 catalyst underwent extremely serious aggregation when using water as a solvent, which was in agreement with the results of XRD analysis. In contrast, the large quantities of Cu particles were homogenously distributed on spent 20ZrCu-Al_2O_3 catalyst (Figure 13 b), while some of them also underwent moderate aggregation (Figure 13 c). The results above demonstrated that addition of ZrO_2 to Cu-Al_2O_3 was beneficial to restrain the aggregation of Cu particles in the reaction process, which was most probably due to the high Cu dispersion and strong interaction between copper and zirconium species on 20ZrCu-Al_2O_3 catalyst.

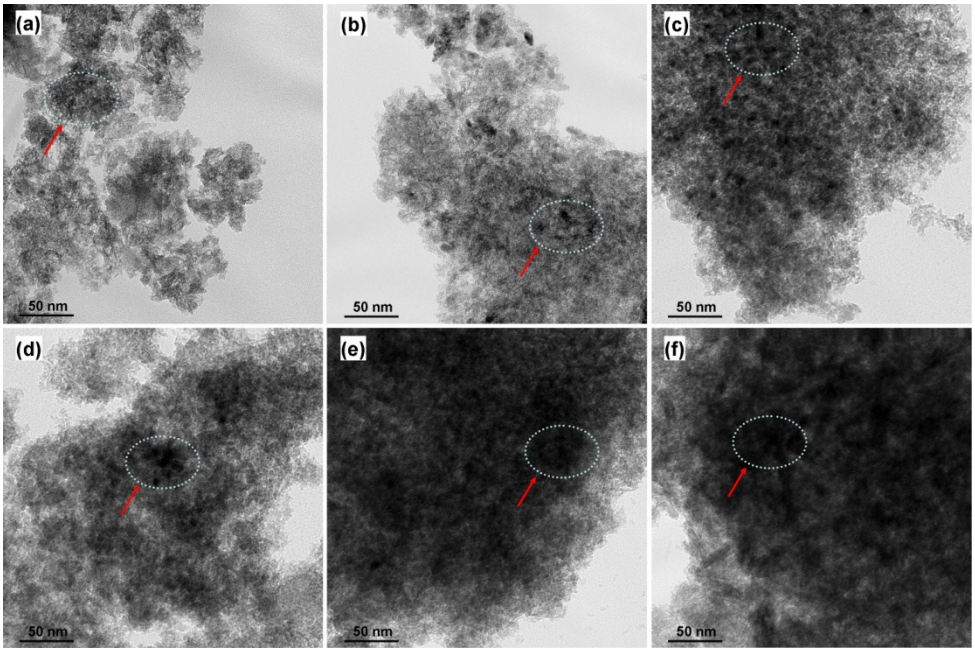

Figure 13. TEM images of the catalysts: (a) fresh 20ZrCu-Al_2O_3; (b) spent 20ZrCu-Al_2O_3 using ethanol as a solvent; (c) spent 20ZrCu-Al_2O_3 using water as a solvent; (d) fresh Cu-Al_2O_3; (e) spent Cu-Al_2O_3 using ethanol as a solvent; (f) spent Cu-Al_2O_3 using water as a solvent.

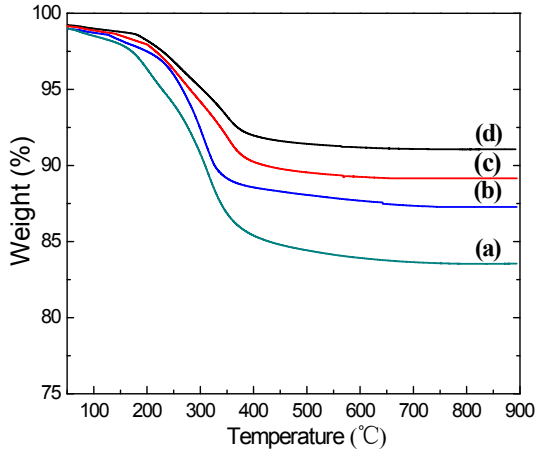

Figure 14. TGA curves of the catalysts: (a) spent 20ZrCu-Al_2O_3 using ethanol as a solvent; (b) spent Cu-Al_2O_3 using ethanol as a solvent; (c) spent 20ZrCu-Al_2O_3 using water as a solvent; (d) spent Cu-Al_2O_3 using water as a solvent.

Apart from the above-mentioned characterization techniques, TGA for the spent catalyst was also carried out. As shown in Figure 14, the weight loss between 50 and 200 ℃ for the spent catalyst was related to the loss of water, while the largest weight loss was presented between 200 and 400 ℃, most likely due to the presence of adsorbed reactant and/or products such as glycerol, 1,2-PDO, acetol and glycerol oligomers on the catalytic surface.[48,49] The presence of adsorbed species on catalytic surface was probably one reason for the loss of catalytic activity. However, it should be noted that the weight losses between 200 and 400 ℃ for spent catalysts in the case of ethanol as a solvent were greater than that when using water as a solvent, suggesting the presence of more adsorbed species on the catalytic surface when ethanol was used as a solvent. In addition, the weight loss between 400 and 900 ℃ for the spent catalyst was very low, showing the lack of carbonaceous deposits on the catalytic surface.[34] But anyway, the results of TGA clearly confirmed that the presence of adsorbed species on catalytic surface might also lead to the deactivation of catalyst.

4. Conclusions

In this work, the ZrO_2-promoted Cu-Al_2O_3 catalysts prepared by co-precipitation method were used for the hydrogenolysis of glycerol to 1,2-PDO in a fixed-bed reactor. The experiment results showed that the introduction of ZrO_2 into Cu-Al_2O_3 could notably enhance the acidity and Cu dispersion on the catalytic surface, which resulted in the increased catalytic activity for glycerol hydrogenolysis. The optimal 20ZrCu-Al_2O_3 catalyst achieved 97.1% glycerol conversion and 95.3% 1,2-propanediol selectivity. The characterization of catalyst revealed that both acid sites and Cu active sites in the catalysts played critical roles in the hydrogenolysis of glycerol to 1,2-propanediol. In addition, the effects of process parameters such as solvent, reaction temperature, operating pressure, glycerol concentration and liquid flow rate on glycerol hydrogenolysis together with the catalyst stability were studied in detail, indicating the ZrO_2-promoted Cu-Al_2O_3 catalyst had the high efficiency for glycerol hydrogenolysis when using ethanol as a solvent. Compared with Cu-Al_2O_3 catalyst, the ZrO_2-promoted Cu-Al_2O_3 catalyst had better stability and prospective for practical application, which was related to the high Cu dispersion and strong interaction between copper and zirconium species. However, the deactivation was observed on the stability test of catalyst. The sintering of Cu particles was the major factor for the deactivation of catalyst. In addition, pore collapse and adsorbed species on the catalytic surface might also result in the loss of catalytic activity.

Acknowledgements

This work was financially supported by the Scientific Research Foundation of Graduate School of Southeast University (YBJJ1530), the National Natural Science Foundation of China (No. 21276050 and 21076044), the Priority Academic Program Development of Jiangsu Higher Education Institutions and Key Laboratory Open Fund of Jiangsu Province (JSBEM201409). The authors gratefully acknowledge these grants.

Notes and references

1 M. Pagliaro, R. Ciriminna, H. Kimura, M. Rossi and C. D. Pina, *Angew. Chem. Int. Ed.*, 2007, **46**, 4434–4440.
2 Y. Nakagawa and K. Tomishige, *Catal. Sci. Technol.*, 2011, **1**, 179–190.
3 A. Corma, S. Iborra and A. Velty, *Chem. Rev.*, 2007, **107**, 2411–2502.
4 R. Rodrigues, N. Isoda, M. Goncalves, F. C. A. Figueiredo, D. Mandelli and W. A. Carvalho, *Chem. Eng. J.*, 2012, **198**, 457–467.
5 S. N. Delgado, D. Yap, L. Vivier and C. Especel, *J. Mol. Catal. A: Chem.*, 2013, **367**, 89–98.
6 N. D. Kim, J. R. Park, D. S. Park, B. K. Kwak and J. Yi, *Green Chem.*, 2012, **14**, 2638–2646.
7 Y. Nakagawa, X. Ning, Y. Amada and K. Tomishige, *Appl. Catal. A: Gen.*, 2012, **433**, 128–134.
8 H. Tan, M. N. Hedhill, Y. Wang, J. Zhang, K. Li, S. Sioud, Z. A. Al-Talla, M. H. Amad, T. Zhan, O. E. Talla and Y. Han, *Catal. Sci. Technol.*, 2013, **3**, 3360–3370.
9 E. van Ryneveld, A. S. Mahomed, P. S. van Heerden, M. J. Green and H. B. Friedrich, *Green Chem.*, 2011, **13**, 1819–1827.
10 V. Rekha, C. Sumana, S. P. Douglas and N. Lingaiah, *Appl. Catal. A: Gen.*, 2015, **491**, 155–162.
11 I. Gandarias, P. L. Arias, J. Requies, M. E. Doukkali and M. B. Güemez, *J. Catal.*, 2011, **282**, 237–247.
12 C. Montassier, J. M. Dumas, P. Granger and J. Barbier, *Appl. Catal. A: Gen.*, 1995, **121**, 231–244.
13 D. Durán-Martín, M. Ojeda, M. L. Granados, J. L. G. Fierro and R. Mariscal, *Catal. Today*, 2013, **210**, 98–105.
14 Z. Wu, Y. Mao, M. Song, X. Yin and M. Zhang, *Catal. Commun.*, 2013, **32**, 52–57.
15 Z. Huang, F. Cui, H. Kang, J. Chen and C. Xia, *Appl. Catal. A: Gen.*, 2009, **366**, 288–298.
16 M. Balaraju, K. Jagadeeswaraiah, P. S. S. Prasad and N. Lingaiah, *Catal. Sci. Technol.*, 2012, **2**, 1967–1976.
17 S. Zhu, X. Gao, Y. Zhu, Y. Zhu, H. Zheng and Y. Li, *J. Catal.*, 2013, **303**, 70–79.
18 E. S. Vasiliadou, E. Heracleous, I. A. Vasalos and A. A. Lemonidou, *Appl. Catal. B: Environ.*, 2009, **92**, 90–99.
19 I. Gandarias, P. L. Arias, J. Requies, M. B. Güemez and J. L. G. Fierro, *Appl. Catal. B: Environ.*, 2010, **97**, 248–256.
20 C. Zhang, T. Liu, H. Wang, F. Wang and X. Pan, *Chem. Eng. J.*, 2011, **174**, 236–241.
21 X. Shi, Y. Wu, P. Li, H. Yi, M. Yang and G. Wang, *Carbohydr. Res.*, 2011, **346**, 480–487.
22 G. Raju, P. S. Reddy and B. M. Reddy, *The open Catal. J.*, 2011, **4**, 83–87.
23 R. V. Sharma, P. Kumar and A. K. Dalai, *Appl. Catal. A: Gen.*, 2014, **477**, 147–156.
24 Y. Zhu, X. Kong, S. Zhu, F. Dong, H. Zheng, Y. Zhu and Y. W. Li, *Appl. Catal. B: Environ.*, 2015, **166**, 551–559.
25 Y. Zhu, X. Kong, D. B. Cao, J. Cui, Y. Zhu and Y. W. Li, *ACS Catal.*, 2014, **4**, 3675−3681.
26 S. L. Hao, W. C. Peng, N. Zhao, F. K. Xiao, W. Wei and Y. H. Sun, *J. Chem. Technol. Biot.*, 2010, **85**, 1499–1503.
27 S. R. Kirumakki, B. G. Shpeizer, G. V. Sagar, K. V. R. Chary and A. Clearfield, *J. Catal.*, 2006, **242**, 319–331.
28 Y. Feng, H. Yin, A. Wang, L. Shen, L. Yu and T. Jiang, *Chem. Eng. J.*, 2011, **168**, 403–412.
29 E. Liu, A. J. Locke, R. L. Frost and W. N. Martens, *J. Mol. Catal. A: Chem.*, 2012, **353**, 95–105.
30 B. Azambre, L. Zenboury, P. D. Costa, S. Capela, S. Carpentier and A. Westermann, *Catal. Today*, 2011, **176**, 242–249.
31 B. Mallesham, P. Sudarsanam, B. V. S. Reddy and B. M. Reddy, *Appl. Catal. B: Environ.*, 2016, **181**, 47–57.
32 C. V. Rode, A. A. Ghalwadkar, R. B. Mane, A. M. Hengne, S. T. Jadkar and N. S. Biradar, *Org. Process Res. Dev.*, 2010, **14**, 1385–1392.
33 E. S. Vasiliadou and A. A. Lemonidou, *Chem. Eng. J.*, 2013, **231**, 103–112.
34 E. S. Vasiliadou, T. M. Eggenhuisen, P. Munnik, P. E. de Jongh, K. P. de Jong and A. A. Lemonidou, *Appl. Catal. B: Environ.*, 2014, **145**, 108–119.
35 R. B. Mane, A. Yamaguchi, A. Malawadkar, M. Shirai and C. V. Rode, *RSC Adv.*, 2013, **3**, 16499–16508.
36 Y. Nakagawa, X. Ning, Y. Amada and K. Tomishige, *Appl. Catal. A: Gen.*, 2012, **433**, 128–134.
37 J. Oh, S. Dash and H. Lee, *Green Chem.*, 2011, **13**, 2004–2007.
38 T. Miyazawa, Y. Kusunoki, K. Kunimori and K. Tomishige, *J. Catal.*, 2006, **240**, 213–221.
39 A. Bienholz, H. Hofmann and P. Claus, *Appl. Catal. A: Gen.*, 2011, **391**, 153–157.
40 I. Gandarias, P. L. Arias, S. G. Fernández, J. Requies, M. E. Doukkali and M. B. Güemez, *Catal. Today*, 2012, **195**, 22–31.
41 S. Xia, L. Zheng, L. Wang, P. Chen and Z. Hou, *RSC Adv.*, 2013, **3**, 16569–16576.
42 L. Gong, Y. Lu, Y. Ding, R. Lin, J. Li, W. Dong, T. Wang and W. Chen, *Appl. Catal. A: Gen.*, 2010, **390**, 119–126.

View Article Online
DOI: 10.1039/C6CY00085A

43 C. Wang, H. Jiang, C. Chen, R. Chen and W. Xing, *Chem. Eng. J.*, 2015, **264**, 344–350.
44 A. Bienholz, F. Schwab and P. Claus, *Green Chem.*, 2010, **12**, 290–295.
45 J. V. H. d'Angelo and A. Z. Francesconi, *J. Chem. Eng. Data*, 2001, **46**, 671-674.
46 V. I. Baranenko and V. S. Kirov, *Atom. Energy*, 1989, **66**, 30–34.
47 T. Li, M. B. Tracka, S. Uddin, J. Casas-Finet, D. J. Jacobs and D. R. Livesay, *PLoS ONE*, 2014, **9**, 1–14.
48 E. S. Vasiliadou and A. A. Lemonidou, *Appl. Catal. A: Gen.*, 2011, **396**, 177–185.
49 W. Suprun, M. Lutecki, T. Haber and H. Papp, *J. Mol. Catal. A: Chem.*, 2009, **309**, 71–78.

View Article Online
DOI: 10.1039/C6CY00085A

Table of contents

The ZrO_2-promoted Cu-Al_2O_3 catalyst presented excellent catalytic activity for the hydrogenolysis of glycerol to 1,2-propanediol.